

CFD Studies of Industrial Gas Turbine Exhaust Diffusers

Kouichi ISHIZAKA¹, Susumu WAKAZONO², Masanori YURI² and Ronald TAKAHASHI³

¹Takasago R. & D. Center, Mitsubishi Heavy Industries Ltd.
2-1-1, Shinhama, Arai-cho, Takasago city, Hyogo, JAPAN

Phone: +81-794-45-6760, FAX: +81-794-45-6947, E-mail: kouichi_ishizaka@mhi.co.jp

²Takasago Machinery Works, Mitsubishi Heavy Industries Ltd.

³Mitsubishi Power Systems, Inc., Miami Office

ABSTRACT

CFD analysis of industrial gas turbine exhaust diffuser was carried out. Purposes of this study are improvement of the performance of exhaust diffuser in consideration of the distortion of the flow of the turbine exit, improvement of the diffuser performance in the big flow rate, and verification of CFD accuracy.

To simulate the diffuser inlet distortion, CFD and experiment was carried out including last stator and rotor.

Predicted turbine exit flow and diffuser pressure recovery is in reasonable good agreement with the measured data.

NOMENCLATURE

C _p	Pressure recovery coefficient
ID	Inner diameter
OD	Outer diameter
L	Diffuser length
ΔR	Diffuser inlet height
A	Diffuser annular area
AR	Area ratio (A ₂ /A ₁)
%Ht	Span fraction
M	Mach number
P _s	Static pressure
P _t	Total pressure
P _a	Atmosphere pressure
LE	Leading edge
TE	Trailing edge
Re	Reynolds number (= ρv ΔR/ μ)
T	Temperature
v	Velocity
μ	Viscosity
ρ	Density

Subscript:

1	Diffuser Inlet
2	Diffuser exit

INTRODUCTION

For industrial gas turbine(Fig.1), the performance of the diffuser and its compactness are one of the item that is in the center of attention. Old way design was largely dependent on the performance map[1]-[4] about basic parameter from the rig test or

fundamental theory. That design neglected the effect of internal structure, flow pattern at turbine exit (ex flow angle and Mach number distribution), unsteadiness, which become common to consider in recent design.

According to that design, it is inevitable to have enough diffuser length, once inlet height is defined that follows much safer design considering the flow distortion and turbulence at the turbine exit.

Recently CFD has been positively used in the design of diffuser [5]-[9]. CFD made it possible to take the effect of the swirl, Mach number distribution at turbine exit, the shape of strut and wall curvature into consideration, although its accuracy is still improved. There are many reports which described CFD accuracy compared with just diffuser test results. (Turbine portion is omitted)

In this study, CFD and experiment is carried out including last stator and rotor. Operating condition of this test is from low subsonic to the transonic. The test results and the accuracy of the CFD prediction are discussed.

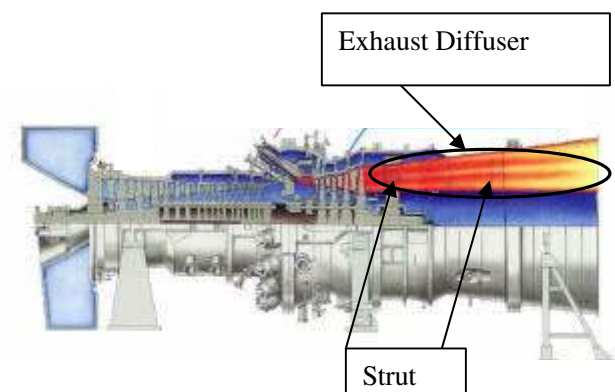


Fig.1 Turbine Exhaust Diffuser

DIFFUSER RIG TEST FACILITY

Figure 2 shows the picture of this test rig. This includes the last stage of the turbine to simulate the flow distributions of the real turbine exit. Figure 3 shows the diffuser geometries for this test.

Table 1 shows the list of the measured points. Table 2 shows the operating conditions for this rig. Turbine exit Mach number is from 0.4 to 0.77 and swirl angle is from -10 to +20 degree. Pressure recovery coefficient of the diffuser is calculated from the diffuser exit wall static pressure and the turbine exit traverse data.

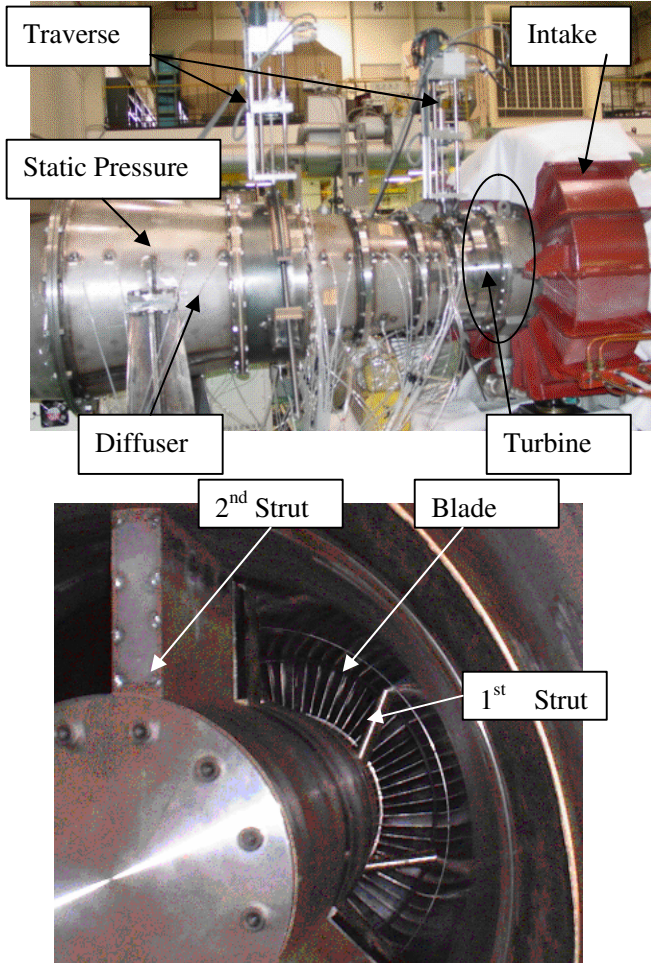


Fig.2 Test Rig

Table 1 List of the Measured Points

Flow rate (Upstream orifice)			1
Turbine Inlet Total Pressure			5
Turbine Inlet Total Temperature			5
Turbine Exit Yaw Angle			3
Turbine Exit Total Pressure			8
Turbine Exit Total Temperature			8
Diffuser Wall Pressure	OD wall	10(Axial)X3(Circumferential)	
	ID wall	7(Axial)X3(Circumferential)	
1st. Strut Surface Pressure	H _{ub}		14
	Mean		18
	Tip		14
2nd Strut Surface Pressure	H _{ub}		17
	Mean		17
	Tip		17
Turbine Exit Traverse			1
Diffuser Exit Traverse			1

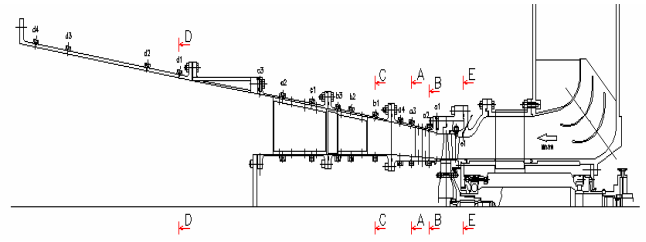


Fig.3 Diffuser Geometries

Table 2 Operating Conditions

Axial Mach	0.4	0.5	0.6			
Swirl (inlet diff)	0	0	-10	0	10	20
Run No.	run019	run018	Run009	Run008	run010	Run011
rpm	12658	15077	19338	17317	14073	10569
G(kg/s)	7.03	8.30	9.80	9.80	10.23	10.60
Axial Mach	0.7		0.63	0.73	0.77	
Swirl (inlet diff)	0	10	20	0	0	0
Run No.	tun014	run013	Run012	Run17	Run015	Run016
rpm	18180	14366	10573	18003	18165	18170
G(kg/s)	11.11	11.53	13.07	10.28	11.86	12.62

NUMERICAL APPROACH

In-house CFD code is applied for this calculation. This code is verified using many cascade and turbine test. Turbulence model is 0-equation model, and wall function is applied for both end-wall and blade surface. Computational domain is form the location of the total pressure probe to the diffuser exit (Fig.4). Total grid counts are about 1 million points. Between each row, 'Mixing-Plane' is applied. Tip clearance of the last blade is modeled to simulate the leakage flow, because total pressure of near end-wall is important for the accuracy of the prediction of the separation. Measured total pressure and temperature at the upstream of the turbine and wall static pressure on the casing is used as boundary conditions for each calculation.

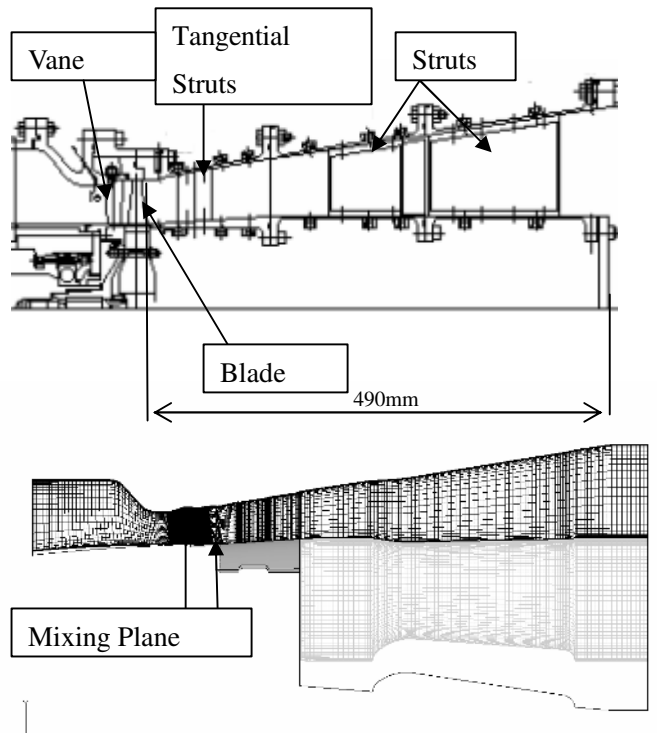


Fig.4 Computational Domain and Grid

CFD VERIFICATION

Before discussing the diffuser performance, numerical results are compared with measured data. Figure 5 shows the comparisons mass flow rate between measured and CFD results. Discrepancy between these data is within 1%.

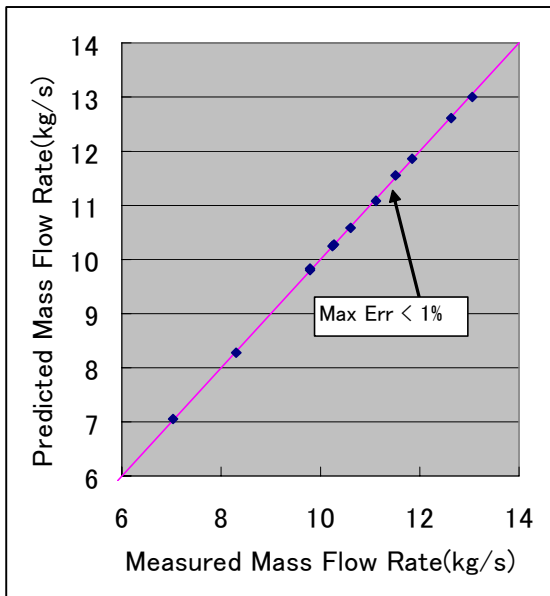


Fig.5 Mass Flow rate of the experiment and CFD

The comparison of measured and CFD wall pressure is shown in Fig. 6(a) and 6(b). Blue line is the predicted pressure (circumferential average) and symbols are the measured pressure. ①-③ mean the measured pressure in different circumferential location and red triangle is the average of ①-③. Predicted wall pressure distribution is in reasonable good agreement with the measured data.

Figure 7 and 8 show the comparisons of the turbine exit flows. Measured data is the Pitot traverse data of both radial and circumferential direction. From 40% Ht to the casing CFD well predicts turbine exit absolute flow angle including tip leakage flow.

Figure 9 shows the comparisons surface Mach number on the strut. Near LE, local supersonic flow appears even if turbine exit Mach number is subsonic.

Figure 10 shows the comparisons pressure recovery of each operating conditions. Blue lines are CFD and red lines are measured data, and same symbol means the same operating condition. CFD is in reasonable good agreement with the measured data.

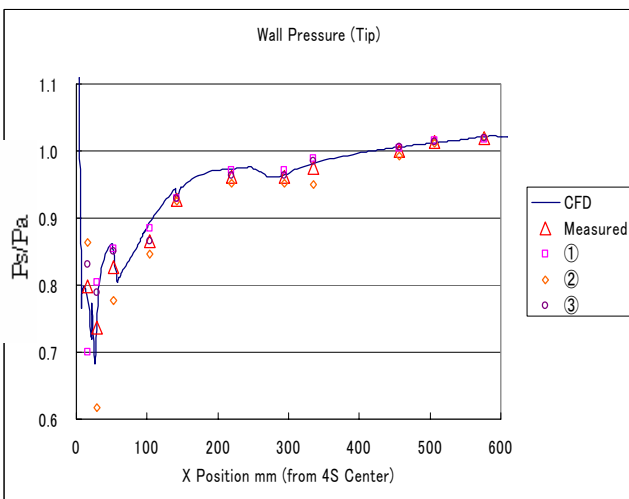


Fig.6 (a) Diffuser Wall Static Pressure at Tip

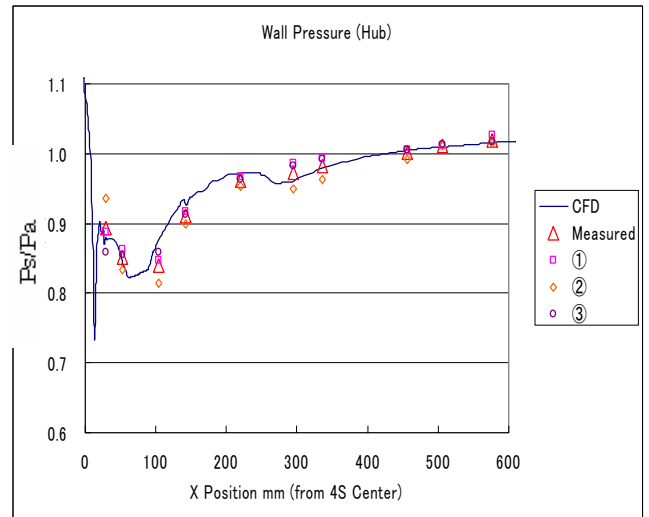


Fig.6 (b) Diffuser Wall Static Pressure at Hub

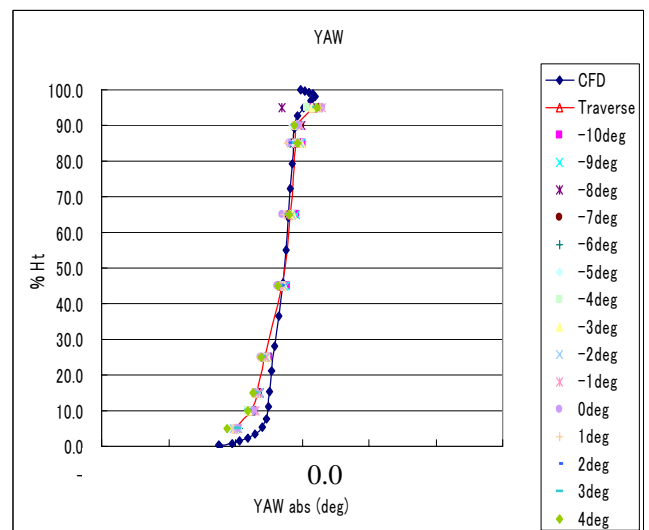


Fig.7 Turbine exit flow angle

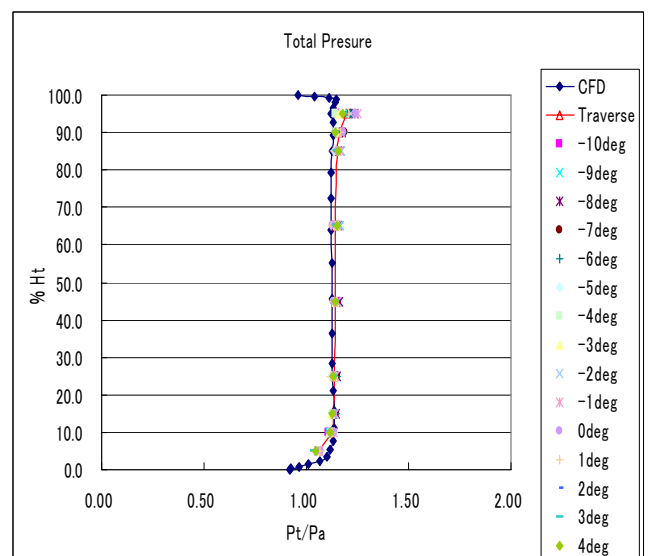


Fig.8 Turbine exit total pressure

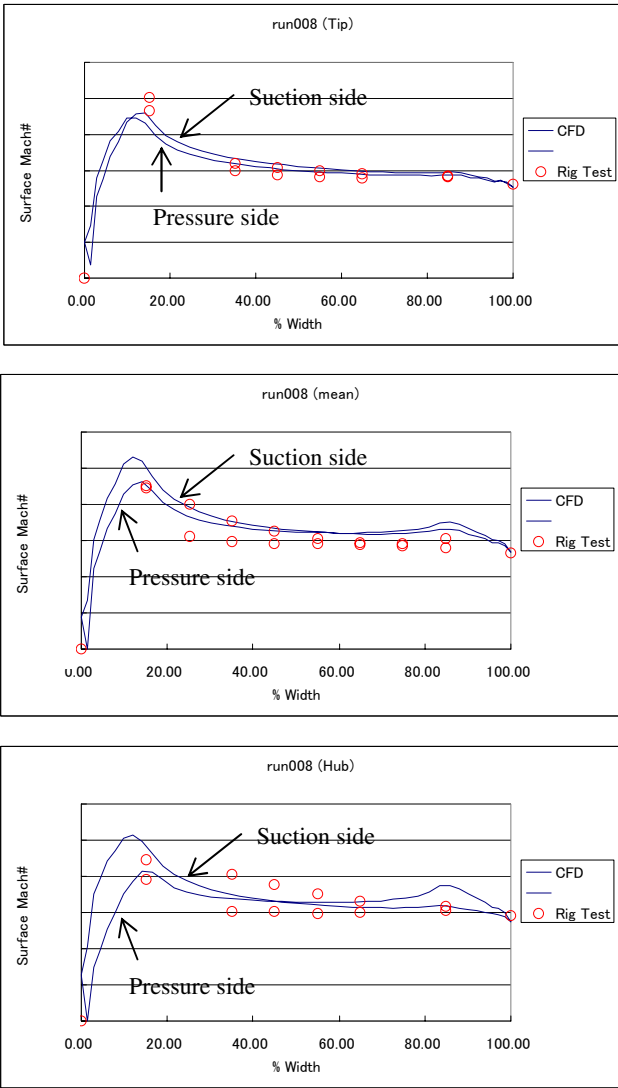


Fig.9 1st Strut Surface Mach number

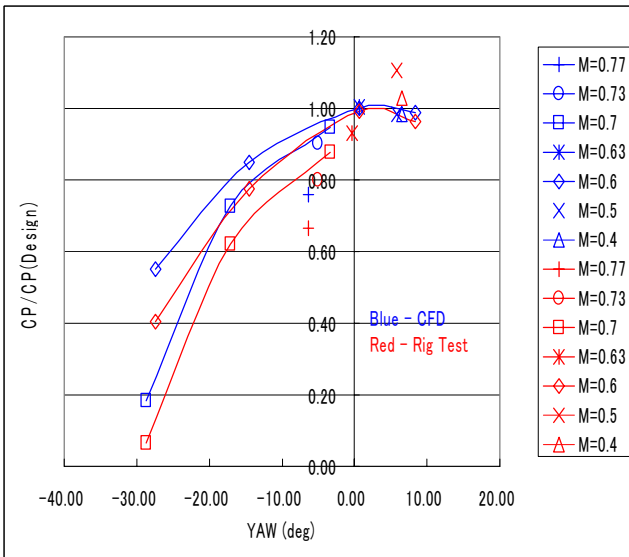


Fig.10 Pressure recovery CP

Pressure recovery of the diffuser that has strut decreases if diffuser inlet Mach number become relatively high (Fig.11). Many experimental data was published about this phenomena (for example [1],[2]). The main reason of this pressure recovery drop is the increasing the pressure loss around the strut. And local supersonic flow or shocks appear.

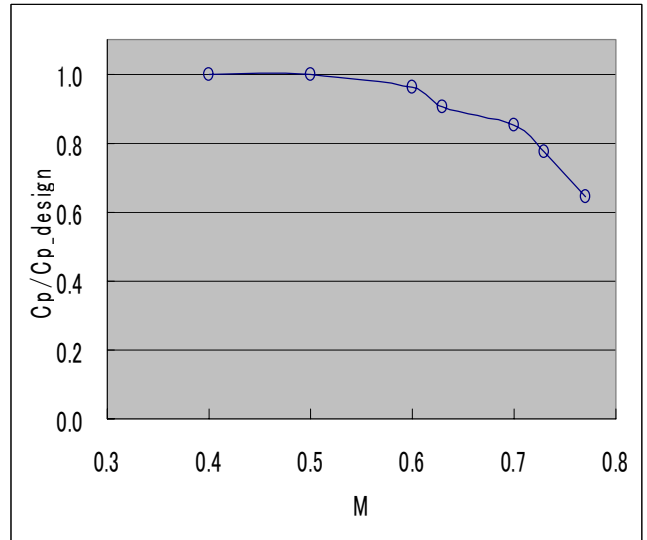


Fig. 11 Cp as a function Mach number

Figure 12 and 14 show the predicted loss coefficient and the pressure recovery factor of each operating condition. Each value is normalized by the designed value. Total Cp is the summation of the Cp of each division. (Total Cp is calculated from positive Cp part minus negative Cp Part.) First, the diffuser is divided by four part s to analyze the local loss coefficient and the pressure recovery. 1: turbine exit to strut inlet, 2: strut (from 5mm upstream of the strut LE to 5mm down stream strut TE), 3: between 1st strut and 2nd strut, 4: 2nd strut to the diffuser exit. (See Fig. 13)

For low Mach number ($M < 0.6$) loss coefficient is almost same value and loss coefficient 2nd strut accounts for 20-30%. For high Mach number ($M > 0.6$), loss coefficient become larger. For large swirl case, loss of between strut become larger, this is because local separation appear between struts. About pressure recovery Cp, for low Mach number, Cp of the 1st strut accounts for 10%. But for high Mach number case, Cp of the 1st strut decreases and $M=0.73$ and $M=0.77$, Cp become negative. With large swirl angle case, loss of 1stStrut increases and Cp decreases because of the separation of the strut.

Figure 15 shows the Mach number contour of meridional plane. This Mach number is area-averaged value in circumferential direction. For $M=0.4$ and 0.5 , flow concentrates in ID-side, and big flow separation appear on the OD wall of down stream of 1st strut.

Figure 16 shows the stream lines that calculated from pitch-wise averaged velocity field. Large separation (not local separation) is seen on ID side for high Mach number and large swirl case, but this separation is not the main reason of the decreasing of pressure recovery. Because Cp of 'Strut-Manhole' and 'Manhole' are still positive.

Figure 17 and 18 are the Mach number contour of S-1(Blade to Blade) plane. Turbine exit Mach number is 0.6 and averaged swirl angle is 0. Near the LE of the strut, maximum Mach number is about 1.15.

Figure 19 and 20 show the span-wise static pressure distributions and total pressure distributions in the diffuser. The distortion of the static pressure at the turbine exit soon change to the flat distribution at the inlet of 1st strut but the distortion of total pressure remains and disturb the diffuser exit flow. This is the reason why the static pressure propagates on the pressure wave of all direction, but total pressure propagates on the entropy wave of streamline direction.

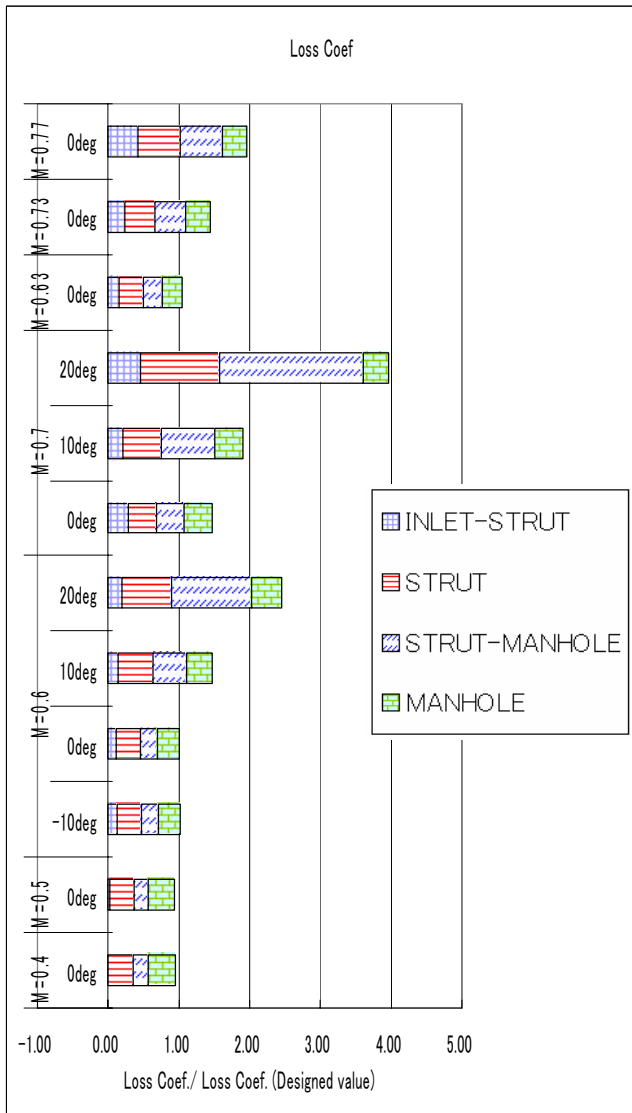


Fig. 12 Pressure loss coefficient

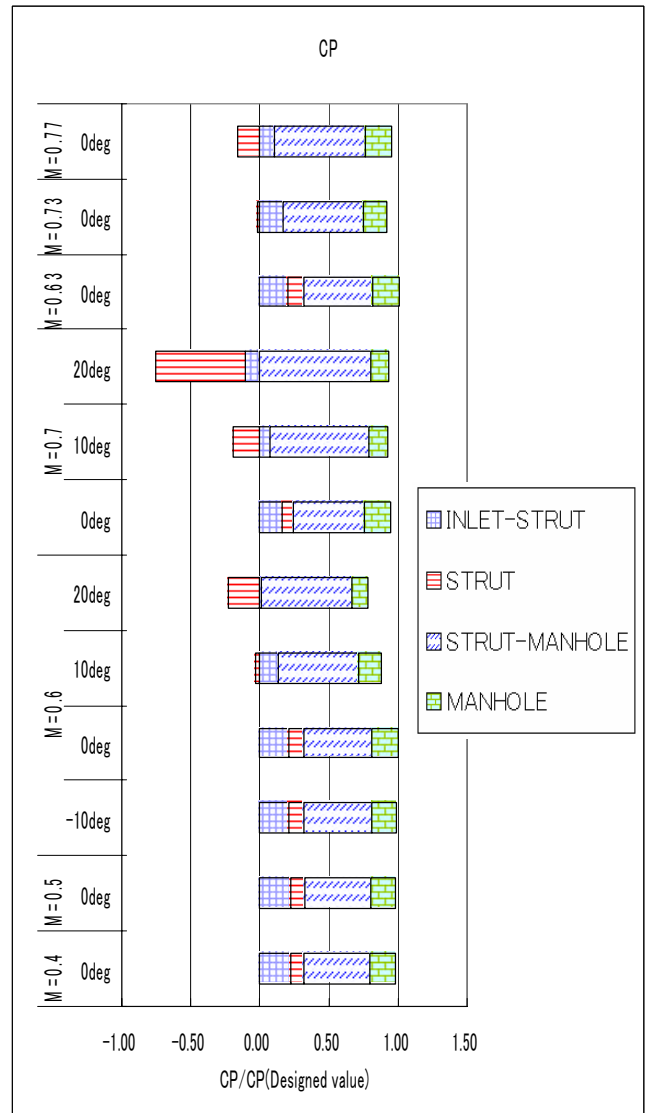


Fig. 14 Pressure Recovery Coefficient

- 1: INLET-STRUT Turbine exit (TE;5mm)-1st Strut inlet (LE-5mm)
- 2: STRUT 1st Strut (LE-5mm)-(TE+5mm)
- 3: STRUT-MANHOLE 1st Strut-2nd Strut(Manhole)
- 4: MANHOLE 2nd Strut (LE-5mm)-Diffuser Exit

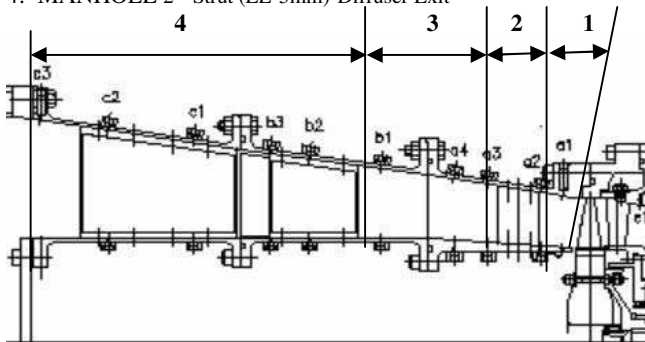


Fig.13 Division of diffuser for analyzing diffuser pressure recovery and losses

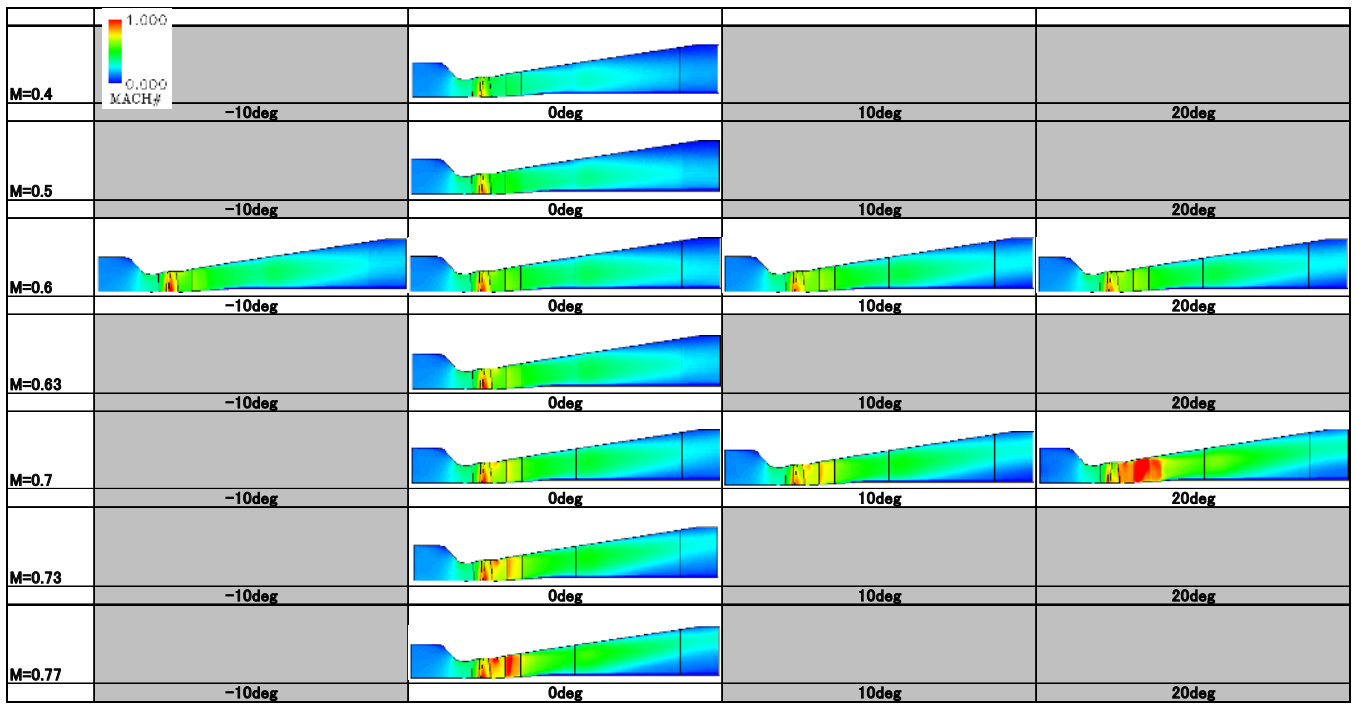


Fig.15 Mach number of meridional plane

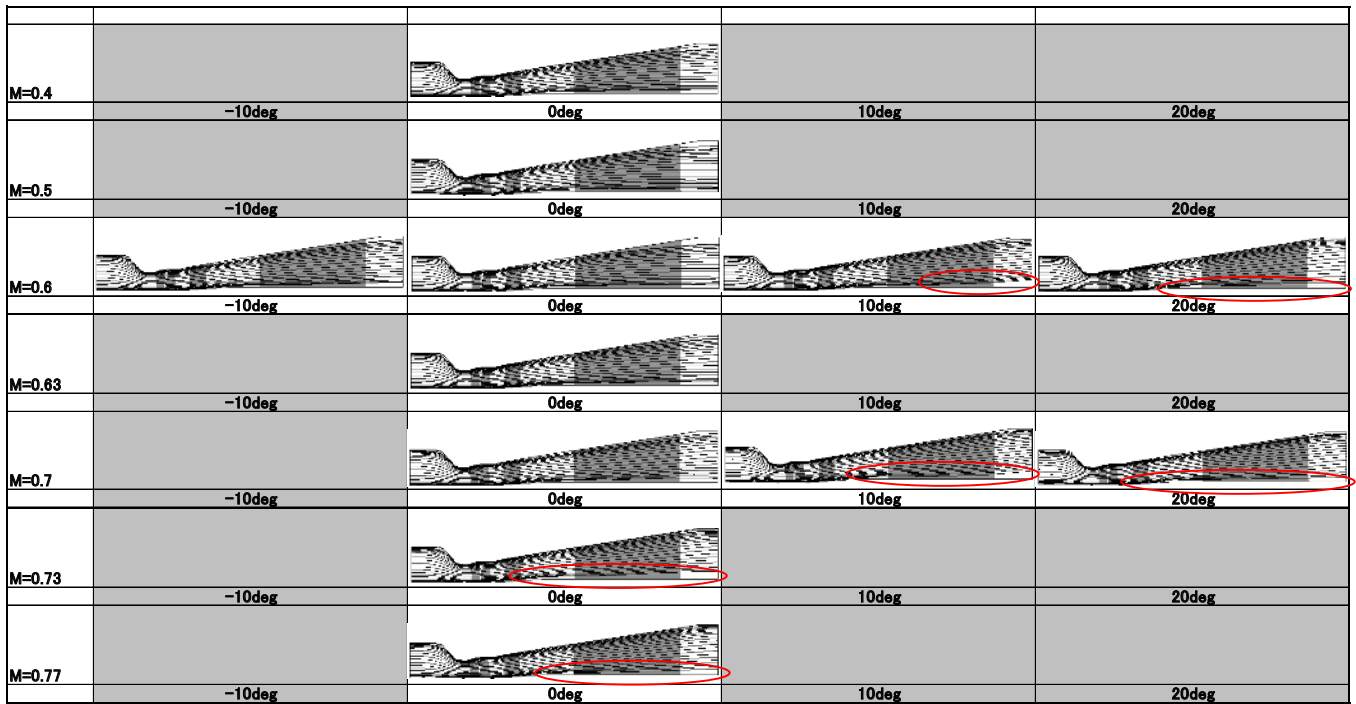
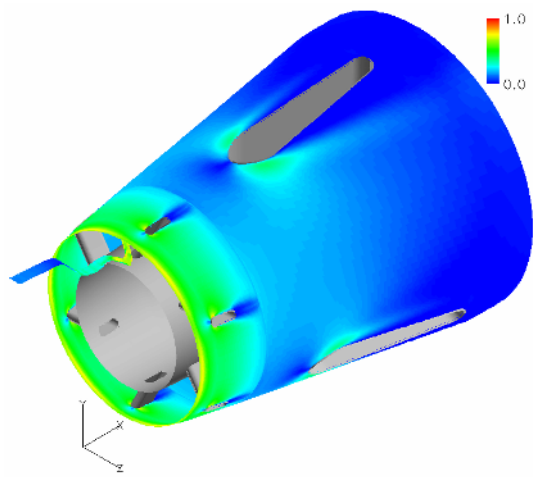
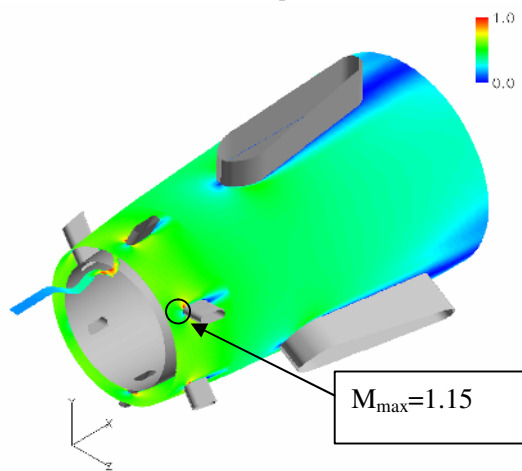


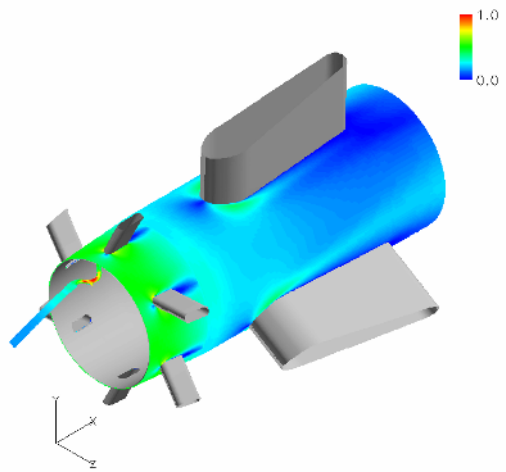
Fig. 16 Stream lines of meridional plane



• Tip

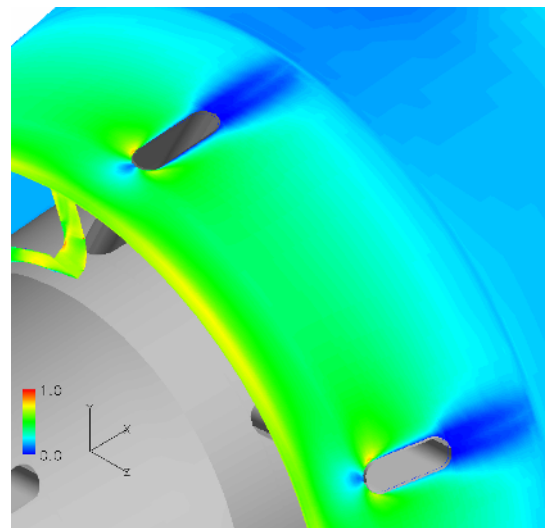


• Mean

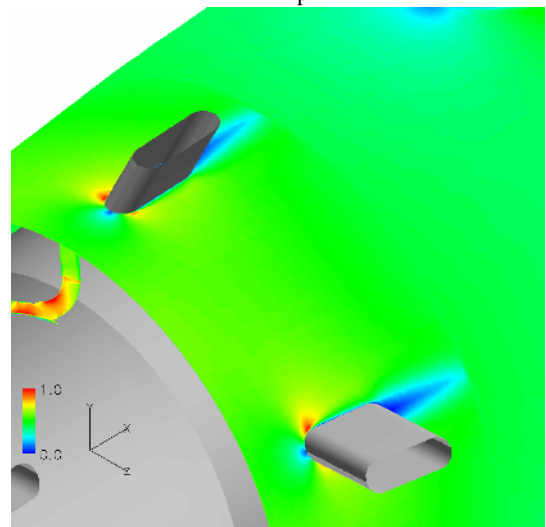


• Hub

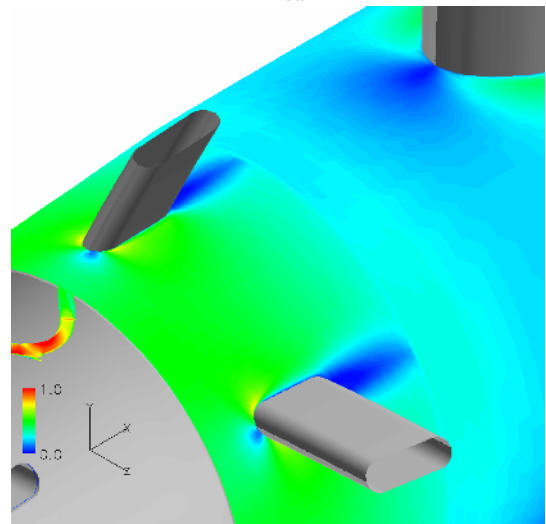
Fig.17 Mach Number Contour : (CASE1)
Axial Mach = 0.6, Swirl = 0



• Tip



• Mean



• Hub

Fig.18 Contours of Mach : Axial Mach = 0.6 ,
Swirl = 0 , Zoom view

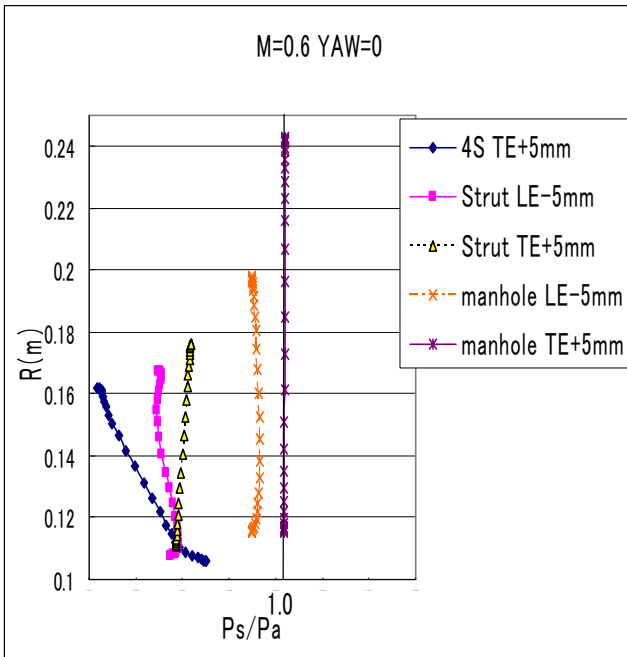


Fig. 19 Static Pressure distributions

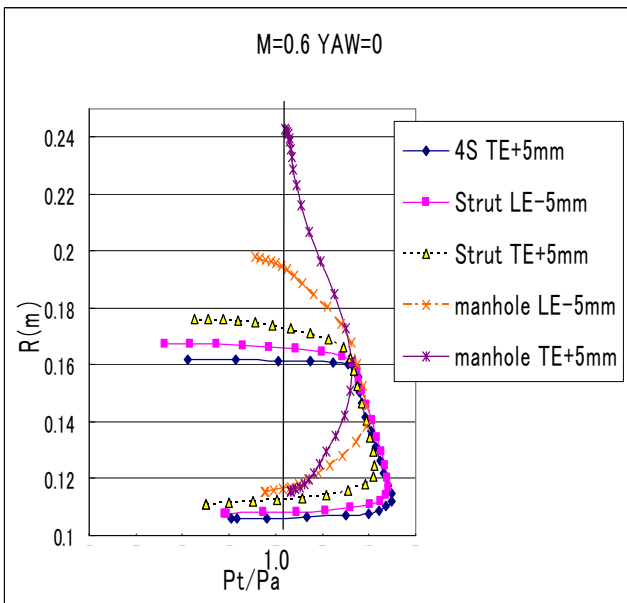


Fig. 20 Total Pressure distributions

CONCLUSIONS

Measurement of the diffuser rig including last stage and CFD were carried out. Operating conditions for each is from $M=0.4$ to 0.77 and Swirl angle is from 10 to -30 degree. From these measurement and CFD, following conclusions are obtained.

Within 20 degree steady CFD well predicts the measured C_p . And for the whole operating condition CFD capture the trend of C_p .

The distortion of the static pressure at the turbine exit soon change to the flat distribution at the inlet of 1^{st} strut but the distortion of total pressure remains and disturb the diffuser exit flow. This is the reason why the static pressure propagates on the pressure wave of all direction, but total pressure propagates on the entropy wave of streamline direction.

Local static pressure recovers to the local total pressure then separation appears and this very depends on turbine exit total pressure distribution.

ACKNOWLEDGEMENT

The authors would like to thank the engineers and technicians in Mitsubishi Heavy Industries, Ltd. for permission to publish this paper.

References

- [1] Japikse, D., and Pampreen, R., "Annular Diffuser Performance for an Automotive Gas Turbine," ASME Paper No.78-GT-147, Apr.1978.
- [2] Johnston, J. P., "Summary of Results of Tests on Short Conical Diffusers with Flow Control Inserts: as of June 1, 1959," Ingersoll-Rand TN No.71, 1959.
- [3] Sovran, G., and Klomp, E.D., "Experimentally Determined Optimum Geometries for Rectilinear Diffusers with Rectangular, Conical or Annular Cross-Section," Fluid Dynamics of Internal Flow, Elsevier Publishing Co., 1967.
- [4] Takehira, A., et al., "An Experimental Study of the Annular Diffusers in Axial-Flow Compressors and Turbines," Japan Society of Mechanical Engineers, Paper No.39, 1977.
- [5] Vassiliev, V., Irmisch, S., Claridge, M. and Richardson, D. P., "Experimental and Numerical Investigation of the Impact of Swirl on the Performance of Industrial Gas Turbines," ASME GT 2003-38424.
- [6] Sultanian, B.K., Nagao, S., Sakamoto, T., "Experimental and Three-Dimensional CFD Investigation in a Gas Turbine Exhaust System," ASME Journal of Engineering for Gas Turbines and Power, April 1999, Vol.121 p.364-374.
- [7] H.-U. Fleige, W. Riess, J. Seume, "Swirl and tip leakage flow interaction with struts in axial diffuser," ASME GT-2002-30491.
- [8] Cunningham, M.H., Birk, A.M., Bartolomeo, W.Di., "Importance of inlet total pressure conditions in evaluating performance of non-symmetric gas turbine exhaust ducts," ASME GT-2002-30499.
- [9] V. Vassiliev, V., Irmisch, S., Florjancic, S., "CFD Analysis of Industrial Gas Turbine Exhaust Diffusers," ASME GT-2002-30597.